Rapid oxidation of paracetamol by Cobalt(II) catalyzed sulfite at alkaline pH

Yanan Yuan, Dan Zhao, Jinjun Li, Feng Wu, Marcello Brigante, Gilles Mailhot

Rapid Oxidation of Paracetamol by Cobalt(II) Catalyzed Sulfite at Alkaline pH

Yanan Yuan[1,2], Dan Zhao[1], Jinjun Li[1], Feng Wu[1*], Marcello Brigante[2], Gilles Mailhot[2*]

[1] Department of Environmental Science, School of Resources and Environmental Science, Wuhan University, Wuhan, 430079, China.

[2] Université Clermont Auvergne, CNRS, SIGMA Clermont, Institut de Chimie de Clermont-Ferrand, F-63000 Clermont–Ferrand, France.

Corresponding Authors: Feng Wu (fengwu@whu.edu.cn) and Gilles Mailhot (gilles.mailhot@uca.fr)

Abstract

In this study we have investigated the efficiency Cobalt (II) (Co(II)) for the activation of sulfite ions following the oxidation of paracetamol used as model contaminants. Physico-chemical parameters that can impact the paracetamol degradation (pH, initial paracetamol concentration, Co(II)/S(IV) molar ratio, oxygen concentration) and contribution of various radicals were investigated in order to elucidate the chemical mechanism. Main results show that the pH is a key factor controlling the efficiency in the system Co(II)/Sulfite. Higher efficiency is observed for pH between 9.0 and 10.0. Increasing S(IV) concentrations, until 1 mM, slightly promoted the degradation of paracetamol. In fact, an excess of sulfite ions inhibits the reaction through the scavenging of $SO_4^{\bullet-}$ and $SO_5^{\bullet-}$. Moreover, degradation efficiency drastically decreases from ~ 85% to less than 5% in absence of oxygen. $SO_4^{\bullet-}$ was confirmed to be the main oxidant responsible for the paracetamol degradation. For the first time we determined the second order rate constant between $SO_4^{\bullet-}$ and paracetamol ($1.33 \pm 0.79 \times 10^9$ M^{-1} s^{-1} (at pH 5) and $6.14 \pm 0.99 \times 10^8$ M^{-1} s^{-1} (at pH 11.0)). Moreover, radical-scavenging experiments also suggest the possible implication of $SO_5^{\bullet-}$. Hence, this work provides a precise understanding of the overall mechanism and a new

promising strategy by using sulfite and transition metal such as Co(II) to promote organic compounds degradation in water under neutral and alkaline pH conditions.

Keywords

Sulfate radical, sulfite ion, cobalt ion, advanced oxidation processes, paracetamol.

1. Introduction

Advanced oxidation processes based on sulfate radical (SR-AOPs) have emerged as a promising method in the field of oxidative decontamination of polluted water and soil [1-3]. Sulfate radical ($SO_4^{\bullet-}$), a strong one-electron oxidant, has relatively high standard redox potential (E^0 = 2.6 V *vs* NHE) with an oxidation potential comparable to or even higher than that of hydroxyl radical [4]. Moreover, $SO_4^{\bullet-}$ can react *via* electron transfer, by addition to C-C double bonds and H-abstraction [5, 6], thus, it is able to oxidize a large number of pollutants such as phenol derivatives and aniline in water [7-9]. $SO_4^{\bullet-}$ can be generated in homogeneous or heterogeneous systems *via* photolysis, thermolysis and radiolysis [10, 11] or *via* transition metal activation of persulfate ($S_2O_8^{2-}$, PS) [7, 12-15] and peroxymonosulfate (SO_5^{2-}, PMS) [16, 17].

In fact, PMS can be activated by various transition metals such as Fe, Mn, Ni and Co in the homogenous systems [1, 18]. Among them, Co and Fe are the most commonly used metal to promote radical formation due to their occurrence in natural media and low cost. Huang and Huang investigated the ability of Co(II) and PMS system to degrade Bisphenol A at pH 7, and achieved an efficient detoxification and mineralization method [19]. A process based on the sulfate radicals generation through iron (Fe(II), Fe(III)) activation of PMS or PS was studied for polychlorinated biphenyls degradation in aqueous system [20]. The high oxidation efficiency and slow rate of consumption of the oxidants make metal-mediated activation system a feasible strategy for degradation of recalcitrant organic compounds. Furthermore, PMS activation using cobalt oxide or cobalt-metal oxide as heterogeneous catalysts also gains significant relevance in water treatment applications [21]. The cobalt oxides such as CoO, CoO_2, CoO(OH), Co_2O_3 and Co_3O_4, Fe–Co mixed oxide nanocatalysts, cobalt oxide

supported on MgO (Co/MgO), on TiO_2 (Co/TiO_2) and Co_3O_4/TiO_2 and combined with other metals were used as efficient heterogeneous catalysts for activation of PMS [22-25]. The most advantage of heterogeneous catalyst is that solid particles can be easily removed from liquid phase and, in some cases, reused.

Recently, sulfite ions were found to react with transition metals such as Fe(II), Fe(III) and Cr(VI) to generate $SO_4^{\bullet-}$ and application for the azo dyes and amine compounds decontamination was tested [17, 26-30].

In our previous work, we reported some novel AOPs using Fe(II)-sulfite, Fe(III)-sulfite, photo-Fe(II)-sulfite system able to produce oxysulfur radicals (including $SO_3^{\bullet-}$, $SO_4^{\bullet-}$ and $SO_5^{\bullet-}$). Combined with the work conducted by other researchers [31-33], the basic chain oxidation mechanisms of oxysulfur radicals generation has been investigated.

In this work, Co(II)-sulfite ions (S(IV)) system has been investigated to promote the paracetamol degradation in water. Paracetamol (PARA) is a widely used analgesic and antipyretic drug and an important material for the manufacturing of azo dyes. PARA was chosen as a target contaminant in this work due to its presence in the environment from several emissions from manufacturing facilities, consumer use and disposal, and hospital waste [34, 35]. The effect of pH, initial PARA concentration, Co(II)/S(IV) molar ratio, the presence of oxygen were investigated. Moreover, the activation mechanism and contribution of reactive oxygen and sulfur species were elucidated by using different kinds of radical scavengers and transient absorption spectroscopy.

2. Materials and Methods

2.1 Chemicals

Cobalt(II) sulfate ($CoSO_4 \cdot 7H_2O$, analytical reagent grade), Cobalt(II) oxide (CoO) and Paracetamol ($C_8H_9NO_2$), were purchased from Sinopharm Chemical Reagent Co., Ltd. Sulfite solutions (from Na_2SO_3, Sinopharm Chemical Reagent Co., Ltd) were prepared just prior to measurements. The radical scavengers tert-butyl alcohol (TBA),

ethanol (EtOH) as well as NaOH and H_2SO_4 which were used to adjust the pH of the solutions, were obtained from Sinopharm Chemical Reagent Co., Ltd. Methanol was HPLC grade and purchased from Fisher Corporation. Ammonium thiocyanate (NH_4SCN) and Methyl isobutyl ketone (MIK) used to determine the concentration of Co(II), were obtained from Sigma, France. All chemicals were used without further purification. Ultrapure water with 18.2 MΩ cm resistivity used in this work was obtained through a water purification system.

2.2 Degradation experiments

All experiments were conducted in a 250 mL open cylindrical reactor cooled by an external jacket water circulation at a constant temperature of 25°C. Appropriate amounts of the PARA, scavengers and Na_2SO_3 were mixed in the solution and the pH was adjusted using a pHS-3C pH meter by adding dilute NaOH and H_2SO_4 until desired value. Each solution was constantly stirred with a Polytetrafluoroethylene (PTFE)-coated magnetic stirrer and purged with air with a fixed flow of 0.8 L min^{-1}.

Each experiment was initialed spiking with Co(II) or CoO into the solution. Samples were withdrawn at fixed interval times and analyzed immediately to determine the remaining concentration of PARA and Co(II). For radical-scavenging experiments, specific concentrations of TBA or EtOH were added to the solutions before Co(II) addition. In order to assess the role of oxygen during Co(II)-sulfite solution were purged by bubbling N_2 (99.99%) or O_2 (99.99%) for 30 min before and throughout the experiment. A dissolved oxygen (DO) meter (8403, AZ Instrument Co. Ltd.) was used to determine the oxygen concentration in solution. During anoxic reaction, the DO was 0.01 mg L^{-1} while for O_2 saturated solution a concentration of 20 mg L^{-1} was determined. All experiments were carried at least two times.

2.3 Chemical analysis

The concentration of PARA was determined using a high-performance liquid chromatography (HPLC) Shimadzu LC-10A system equipped with UV-vis detector (SPD-10AV; Shimadzu) and an ODS-C18 column (25 cm × 4.6 mm, 5 μm; Shimadzu, Kyoto, Japan). The separation was warried out using methanol:water (25:75 v/v) as

isocratic mobile phase at a flow rate of 1.0 mL min^{-1}. The detector was set at 241 nm. The concentration of Co(II) in solution was determined by Methyl isobutyl ketone and Ammonium thiocyanate (see Supplementary material for the method description and Fig. S1) [36]. An optical-fiber coupled to a spectrophotometer (UV-1601 Shimadzu, Japan) was used to scan the UV–vis absorption spectra of Co(II)-SO_3^{2-} complex.

For $SO_4^{\bullet-}$ reactivity a laser flash photolysis (LFP) system was used with 266 nm excitation following the procedure reported by Wu at al. [15]. Analysis of transient decay and second order rate constant determination (using PARA concentrations from 0 to 0.1 mM) were determined at 470 nm corresponding to the maximum absorption of $SO_4^{\bullet-}$. The second order rate constants were determined at pH 5.0 and 11.0 corresponding to the molecular and deprotonated forms respectively of PARA (pKa = 9.5).

3. Results and discussion

3.1 Effect of initial pH on paracetamol degradation

The effect of the initial pH on the Co(II)+S(IV) system oxidation of PARA was investigated from 3.0 to 11.0. The initial concentrations of Co(II) and SO_3^{2-} were 0.1 mM and 1.0 mM, respectively and during the reaction, air (otherwise stated) was constantly bubbled at a flow rate of 0.8 L min^{-1}. The PARA degradation shows a strong pH-dependence as illustrated in Fig. 1A. Despite a negligible degradation at relatively acidic values (pH 3.0 – 5.0), PARA degradation is enhanced from pH 5.0 to pH 10.0 while a decrease is observed at pH 11.0. It is interesting to observe that degradation efficiency between pH 3.0 and 10 is strongly correlated to the HSO_3^-/SO_3^{2-} speciation in solution (pKa = 7.2) as shown in Fig. 1B in which degradation of PARA after 30 min at different pH values is correlated to the concentration of SO_3^{2-} in solution. However, at pH 11, the inhibition of PARA degradation can be attributed to the formation of insoluble Cobalt-hydroxide ($Co(OH)_2$) complex that is expected to precipitate in solution [37].

Moreover, it has been reported that deprotonated complexes (Co(II)−OH), which

is more reactive toward SO_3^{2-} compared to HSO_3^- would be formed at alkaline pH values (R1) leading to the formation of a Co(II)−SO_3 complex [27]. Co(II)−SO_3 could be oxidized to Co(III)−SO_3^+ complex in the presence of dissolved oxygen as reported in different works (R2 and R3) [38]. $SO_3^{\bullet-}$ could be generated during the redox reaction between the Co(III)-SO_3^+ complex and SO_3^{2-} (R4).

UV–vis absorption spectra of Co(II), S(IV), Co(II) and S(IV) during the reaction (Fig. S1) were acquired to investigate the complexation between Co(II) and S(IV). The result showed that: only Co(II) or S(IV) at pH 9.0 did not show absorption in the range 250-600 nm. However, when S(IV) was added to the solution containing 0.1 mM Co(II) an absorption band absorbing up to ~ 600 nm is present. The presence of this new absorption band demonstrates that the Co(II)-S(IV) complex could be formed and decreasing in the absorption during time proved the reaction between Co(II) and S(IV), and corresponding depletion of S(IV).

$$Co(II) + H_2O \rightarrow Co(II) - OH \qquad \text{alkaline pH} \qquad \text{(R1)}$$

$$Co(II) - OH + SO_3^{2-} \rightarrow Co(II) - SO_3 + H_2O \qquad \text{(R2)}$$

$$Co(II) - SO_3 + O_2 \rightarrow Co(III) - SO_3^+ \qquad \text{(R3)}$$

$$Co(III) - SO_3^+ + SO_3^{2-} \rightarrow Co(II) - SO_3 + SO_3^{\bullet-} \qquad \text{(R4)}$$

The pH represents also a key factor influencing the $SO_3^{\bullet-}$ reactivity in water. In fact, the primary step is the oxygen-mediated oxidation of $SO_3^{\bullet-}$ to $SO_5^{\bullet-}$ (R5), this latter can react with HSO_3^-/SO_3^{2-} leading to the formation of $SO_3^{\bullet-}$ and $SO_4^{\bullet-}$ (R6-R9).

As reported in R6 and R8, $SO_5^{\bullet-}$ could react with SO_3^{2-} to generate $SO_3^{\bullet-}$ and $SO_4^{\bullet-}$ at a rate constant around 10^5–10^6. $SO_4^{\bullet-}$ could react with PARA or with SO_3^{2-} leading to the generation $SO_3^{\bullet-}$ (R10), then a $SO_x^{\bullet-}$ ($SO_3^{\bullet-}$, $SO_4^{\bullet-}$ and $SO_5^{\bullet-}$) cycle can be achieved. However, in the presence of HSO_3^- (acidic conditions), $SO_5^{\bullet-}$ reacts with HSO_3^- to generate $SO_4^{\bullet-}$/$SO_3^{\bullet-}$ with a relatively shower rate constants (R7 and R9)

compared to the reactivity with SO_3^{2-}. The overall reaction rate between $SO_5^{\bullet-}$ and SO_3^{2-} is ~1–2 orders of magnitude higher than between $SO_5^{\bullet-}$ and HSO_3^-.

$SO_3^{\bullet-} + O_2 \rightarrow SO_5^{\bullet-}$ k= (1.5–2.5) × 10^9 $M^{-1}s^{-1}$ [39, 40] (R5)

$SO_5^{\bullet-} + SO_3^{2-} \rightarrow SO_4^{2-} + SO_4^{\bullet-}$ k= 9 × 10^6 $M^{-1}s^{-1}$ [41] (R6)

$SO_5^{\bullet-} + HSO_3^- \rightarrow HSO_4^- + SO_4^{\bullet-}$ k= 2.5 × 10^4 $M^{-1}s^{-1}$ [42] (R7)

$SO_5^{\bullet-} + SO_3^{2-} \rightarrow SO_5^{2-} + SO_3^{\bullet-}$ k= 3.8 × 10^6 $M^{-1}s^{-1}$ [41] (R8)

$SO_5^{\bullet-} + HSO_3^- \rightarrow HSO_5^- + SO_3^{\bullet-}$ k= 7.5 × 10^4 $M^{-1}s^{-1}$ [42] (R9)

$SO_4^{\bullet-} + SO_3^{2-} \rightarrow SO_4^{2-} + SO_3^{\bullet-}$ k = 5.7 × 10^8 $M^{-1}s^{-1}$ [41] (R10)

$SO_4^{\bullet-} + HSO_3^- \rightarrow HSO_4^- + SO_3^{\bullet-}$ k= 7.5 × 10^8 $M^{-1}s^{-1}$ [43] (R11)

3.2 S(IV) and Co(II) effect on the PARA degradation

Different amounts of Co(II) were used to investigate the effect of Co(II) concentration on the PARA removal at pH 9.0 (Fig. 2A). When experiments were conducted using a Co(II) concentration between 0.05 and 0.15 mM and a fixed sulfite concentration of 1.0 mM, no significant differences were observed on the PARA degradation profile. One of reasons explaining the slightly effect of Co(II) concentration may be the fast recycle of Co(II) and Co(III) in the presence of a stoichiometry excess of S(IV) concentrations in aerated solution (R3-R4). Moreover, when the concentration of Co(II) was monitored during the reaction (see the Supplementary material for the method description), it was found that its concentration was nearly stable (Fig. S3). Such results suggest that in the presence of enough sulfite in solution, the cobalt recycle could achieved very fast leading to the generation of $SO_3^{\bullet-}$ at the same time. Even the addition of Co(II) didn't play a relevant role on the paracetamol degradation, but for the sake of feasibility and accuracy, 0.1 mM Co(II) was employed during all experiments, as when the experiments were conducted under low concentration of Co(II) such as 0.05 mM, the repeatability could not be ensured

every time.

The dependence of the PARA degradation on the initial concentration of S(IV) was also investigated (Fig. 2B). An increase in S(IV) concentration (between 0.5 to 1 mM) accelerate the PARA degradation being , through Co(II) reactivity, a source of $SO_3^{\bullet-}$. However, at higher sulfite ions concentrations (2 mM) there is no more enhancement of PARA degradation and this effect could be attributed to the reactivity competition of $SO_4^{\bullet-}/SO_5^{\bullet-}$ between PARA and SO_3^{2-} (R8 and R10). Hence, the balance between S(IV) concentration and its catalytic character is a key factor for the oxidative system efficiency.

In all these experiments (Fig. 2) it is impossible to obtain more than 90% of PARA degradation. This observation is certainly due to a competition reaction of the sulfate radicals on PARA, the excess of sulfite and the degradation products of PARA. After a short period of time sulfate radicals react no more on paracetamol due to its low concentration.

3.3 Effect of O_2

The effect of oxygen concentration on the PARA degradation using 0.1 mM of Co(II) and 1 mM of S(IV) was investigated comparing results from aerated and nitrogen-purged solutions. When experiment was conducted in aerated solution (under air bubbling), a PARA degradation plateau was reached after first 10 min corresponding to ~82% of degradation (Fig. 3). However, under nitrogen-saturated solution, the efficiency dropped to less than 8% confirming that oxygen is a crucial parameter. Oxygen strongly favors the degradation of pollutant through $SO_3^{\bullet-}$oxidation into $SO_5^{\bullet-}$ that undergo further reaction to form $SO_4^{\bullet-}$ in the solution (R5-R7).

3.4 Radical species involvement

The second order rate constants of sulfate radical with molecular and deprotonated PARA (at pH 9.0, pH used in our experiments, about 25 % of PARA is under deprotonated form) were determined from the linear fit of pseudo-first order decay monitored at 470 nm (corresponding to the maximum absorption of sulfate radical) *vs*

concentration of PARA in solution (Fig. S4). The second order rate constant was estimated to be $1.33 \pm 0.79 \times 10^9$ M^{-1} s^{-1} (at pH 5) and $6.14 \pm 0.99 \times 10^8$ M^{-1} s^{-1} (at pH 11.0) corresponding respectively to the molecular and deprotonated form, on the phenol group, of PARA.

To shed light onto radical mechanism involved in such system, EtOH and TBA were used as radical scavengers. This competition kinetic approach is based on the different second-order rate constant with $HO^{\bullet}$ and $SO_4^{\bullet-}$ ($k_{TBA,HO^{\bullet}} = 6.0 \times 10^8$ M^{-1} s^{-1} [44] which is nearly three orders of magnitude higher than $k_{TBA,SO_4^{\bullet-}} = 8.5 \times 10^5$ M^{-1} s^{-1} [45] and $k_{EtOH,HO^{\bullet}} = 1.9 \times 10^9$ M^{-1} s^{-1} [44], $k_{EtOH,SO_4^{\bullet-}} = 5.6 \times 10^7$ M^{-1} s^{-1} [41]). In the presence of TBA (up to 6 mM) no effect was observed on the PARA degradation [Fig. S5] indicating that hydroxyl radical are not generated using Co(II) 0.1 mM and SO_3^{2-} 1 mM at pH 9.0. Indeed, if hydroxyl radical were produced in the system, addition of 1 mM TBA should be scavenged about 98 % $HO^{\bullet}$ reducing drastically the PARA degradation. However, when EtOH was used as radical scavenger in solution (Fig. 4) PARA degradation rate and efficiency (after 30 min) were modified. In the presence of 500 mM of EtOH, a complete inhibition of PARA degradation should be expected on the basis of second order rate constant reported before. But, PARA is still degraded with ~ 29% of disappearance after 30 min. Such trend could be explained considering the possible involvement of $SO_5^{\bullet-}$ during PARA degradation. In fact, EtOH is not able to scavenge strongly $SO_5^{\bullet-}$ due to the very low rate constant ($k_{EtOH,SO_5^{\bullet-}} < 10^3$ M^{-1} s^{-1} [46]).

Such results suggest that $SO_4^{\bullet-}$ represent the main radical leading to the degradation, but also possible implication of $SO_5^{\bullet-}$ during degradation of PARA is possible.

3.5 Heterogeneous reaction between CoO and SO_3^{2-}

Cobalt oxide such as CoO, CoO_2, CoO(OH), Co_2O_3 and Co_3O_4 were usually used to react with PMS to oxidize different kinds of organic pollutants [24]. Experiments to prove the efficiency of sulfite activation by CoO were conducted at pH 9.0 with the

paracetamol concentration of 10 μM and SO_3^{2-} at 1.0 mM. As shown in Fig. 5, when 0.1 mM and 1.0 mM CoO were added to the solution, the degradation efficiency were 32.9% and 71.7%, after 30 min respectively, which indicates that CoO exhibit a good catalytic activity. One of heterogeneous catalysts advantages belong to their stability and their reusability as catalyst. However, oxide can easily agglomerate during catalytic reaction, resulting in the reduction of catalytic performance [47], also cobalt ion leaching and dissolving problem can cause the same potential environmental and health problem as homogeneous catalysts do. As reported in Fig. 5 and Fig. 2A, the initial degradation rate is completely different in the two systems, very fast with soluble Co(II) and much slower with CoO. This observation shows that the reactivity of sulfite with cobalt is efficient in homogeneous phase and so with cobalt oxide a first process of solubilisation seems necessary.

3.6 Sequential experiments for high concentration paracetamol

Sequential experiments were performed with multiple additions of S(IV) to enhance the degradation of high concentration of paracetamol in this Co(II)-S(IV) system. In the experiment, the concentration of paracetamol was 500 μM, Co(II) was 0.5 mM, and the initial pH value of solution was adjusted to 9.0 and then controlled during the whole reaction. 5 mM S(IV) was added to the solution at the beginning, while 0.5 mM were spiked every 20 min. After 200 min of reaction, (Fig. S6) nearly complete PARA degradation was archived. Compared to Co(II), which is recycled during the reaction, sulfite is consumed as transforms into $SO_3^{\bullet-}$ and subsequently into SO_4^{2-}. So due to the depletion of S(IV), multiple additional sulfite is necessary to promote sequential treatment.

4. Conclusion

Our results showed the high efficiency of this Co(II)-S(IV) system using PARA as organic pollutant model in aqueous solution at alkaline pH. In this system, the degradation of paracetamol depend on initial concentrations of S(IV) and strongly the pH. In fact, it is clear that dissolved oxygen plays a crucial role allowing the oxysulfure

radicals oxidation to initiate the reaction. The results of radical scavenger experiments demonstrate that $SO_4^{\bullet-}$ and also $SO_5^{\bullet-}$ (to a lesser extent) are involved during the paracetamol degradation. Furthermore, heterogeneous catalyst CoO also could react with sulfite to degrade paracetamol to a large extent. In general, this research work provides a new promising strategy by using sulfite and transition metal Co(II) to degrade organic compounds in wastewater under alkaline environment. One of the perspectives of this work is to perform same experiments with other metals in order to assess their ability to promote the radical generation from sulfite under dark and light conditions.

Acknowledgement

This work was supported by the National Natural Science Foundation of China (NSFC-CNRS_ PRC No. 21711530144 and CNRS No. 270437) .This work was also supported by the "Federation des Recherches en Environnement" through the CPER "Environnement" founded by the "Région Auvergne," the French government and FEDER from European community. The authors gratefully acknowledge financial support from China Scholarship Council provided to Yanan Yuan to study at the University Clermont Auvergne in Clermont-Ferrand, France.

References

[1] G.P. Anipsitakis, D.D. Dionysiou, Environ. Sci. Technol. 37 (2003) 4790-4797.
[2] P. Shukla, H. Sun, S. Wang, H.M. Ang, M.O. Tadé, Catal. Today 175 (2011) 380-385.
[3] Y. Zuo, J. Zhan, T. Wu, J. Atmos. Chem. 50 (2005) 195-210.
[4] P. Neta, R.E. Huie, A.B. Ross, J. Phys. Chem. Ref. Data 17 (1988) 1027-1284.
[5] H.V. Lutze, S. Bircher, I. Rapp, N. Kerlin, R. Bakkour, M. Geisler, C. von Sonntag, T.C. Schmidt, Environ. Sci. Technol. 49 (2015) 1673-1680.
[6] Y. Ren, L. Lin, J. Ma, J. Yang, J. Feng, Z. Fan, Appl. Catal., B 165 (2015) 572-578.
[7] G.P. Anipsitakis, D.D. Dionysiou, M.A. Gonzalez, Environ. Sci. Technol. 40 (2006) 1000-1007.
[8] Y.-T. Lin, C. Liang, J.-H. Chen, Chemosphere 82 (2011) 1168-1172.
[9] X. Xie, Y. Zhang, W. Huang, S. Huang, J. Environ. Sci. 24 (2012) 821-826.
[10] M.G. Antoniou, A.A. de la Cruz, D.D. Dionysiou, Appl. Catal., B 96 (2010) 290-298.
[11] J. Criquet, N. Karpel Vel Leitner, Chem. Eng. J. 169 (2011) 258-262.
[12] H. Guo, N. Gao, Y. Yang, Y. Zhang, Chem. Eng. J. 292 (2016) 82-91.
[13] L.W. Matzek, K.E. Carter, Chemosphere 151 (2016) 178-188.
[14] Y. Wu, R. Prulho, M. Brigante, W. Dong, K. Hanna, G. Mailhot, J. Hazard. Mater. 322, Part B (2017) 380-386.
[15] Y. Wu, A. Bianco, M. Brigante, W. Dong, P. de Sainte-Claire, K. Hanna, G. Mailhot, Environ. Sci. Technol. 49 (2015) 14343-14349.
[16] C. Qi, X. Liu, J. Ma, C. Lin, X. Li, H. Zhang, Chemosphere 151 (2016) 280-288.
[17] T. Zhang, H. Zhu, J.-P. Croué, Environ. Sci. Technol. 47 (2013) 2784-2791.
[18] A.B. Kurukutla, P.S.S. Kumar, S. Anandan, T. Sivasankar, Environ. Eng. Sci. 32 (2014) 129-140.
[19] Y.-F. Huang, Y.-H. Huang, J. Hazard. Mater. 167 (2009) 418-426.
[20] A. Rastogi, S.R. Al-Abed, D.D. Dionysiou, Appl. Catal., B 85 (2009) 171-179.
[21] F. Ghanbari, M. Moradi, Chem. Eng. J. 310, Part 1 (2017) 41-62.
[22] H. Liang, H. Sun, A. Patel, P. Shukla, Z.H. Zhu, S. Wang, Appl. Catal., B 127 (2012) 330-335.
[23] M. Stoyanova, I. Slavova, S. Christoskova, V. Ivanova, Appl. Catal. A 476 (2014) 121-132.
[24] Y. Wang, L. Zhou, X. Duan, H. Sun, E.L. Tin, W. Jin, S. Wang, Catal. Today 258 (2015) 576-584.
[25] Y. Zhu, S. Chen, X. Quan, Y. Zhang, RSC Adv. 3 (2013) 520-525.
[26] L. Chen, X. Peng, J. Liu, J. Li, F. Wu, Ind. Eng. Chem. Res. 51 (2012) 13632-13638.

[27] Z. Liu, S. Yang, Y. Yuan, J. Xu, Y. Zhu, J. Li, F. Wu, J. Hazard. Mater. 324, Part B (2017) 583-592.
[28] Y. Yuan, S. Yang, D. Zhou, F. Wu, J. Hazard. Mater. 307 (2016) 294-301.
[29] D. Zhou, L. Chen, C. Zhang, Y. Yu, L. Zhang, F. Wu, Water Res. 57 (2014) 87-95.
[30] D. Zhou, Y. Yuan, S. Yang, H. Gao, L. Chen, J. Sulfur Chem. 36 (2015) 373-384.
[31] D.T.F. Kuo, D.W. Kirk, C.Q. Jia, J. Sulfur Chem. 27 (2006) 461-530.
[32] Y. Zuo, Geochim. Cosmochim. Acta 59 (1995) 3123-3130.
[33] Y. Zuo, J. Zhan, Atmos. Environ. 39 (2005) 27-37.
[34] M.J. Benotti, R.A. Trenholm, B.J. Vanderford, J.C. Holady, B.D. Stanford, S.A. Snyder, Environ. Sci. Technol. 43 (2009) 597-603.
[35] L. Zhang, J. Hu, R. Zhu, Q. Zhou, J. Chen, Appl. Microbiol. Biotechnol. 97 (2013) 3687-3698.
[36] D. Katakis, A.O. Allen, J. Phys. Chem. 68 (1964) 1359-1362.
[37] K.H. Chan, W. Chu, Water Res. 43 (2009) 2513-2521.
[38] W. Pasiuk-Bronikowska, T. Bronikowski, M. Ulejczyk, Environ. Sci. Technol. 26 (1992) 1976-1981.
[39] R.E. Huie, P. Neta, J. Phys. Chem. 88 (1984) 5665-5669.
[40] G.V. Buxton, S. McGowan, G.A. Salmon, J.E. Williams, N.D. Wood, Atmos. Environ. 30 (1996) 2483-2493.
[41] U. Deister, P. Warneck, J. Phys. Chem. 94 (1990) 2191-2198.
[42] R.E. Huie, P. Neta, Atmos. Environ. 21 (1987) 1743-1747.
[43] P.H. Wine, Y. Tang, R.P. Thorn, J.R. Wells, D.D. Davis, J. Geophys. Res. 94 (1989) 1085-1094.
[44] G.V. Buxton, C.L. Greenstock, W.P. Helman, A.B. Ross, J. Phys. Chem. Ref. Data 17 (1988) 513-886.
[45] C.L. Clifton, R.E. Huie, Int. J. Chem. Kinet. 21 (1989) 677-687.
[46] E. Hayon, A. Treinin, J. Wilf, J. Am. Chem. Soc. 94 (1972) 47-57.
[47] J. Deng, S. Feng, K. Zhang, J. Li, H. Wang, T. Zhang, X. Ma, Chem. Eng. J. 308 (2017) 505-515.

Figures Captions

Fig. 1: Effect of initial pH values on PARA degradation. Condition: $[PARA]_0$ = 10 μM, $[Co(II)]_0$ = 0.1 mM, $[Na_2SO_3]_0$ = 1.0 mM, T = 25°C, F_{air} = 0.8 L min^{-1}.

Fig. 2: Effect of (A) Co(II) and (B) S(IV) concentrations on PARA degradation. Condition: $[PARA]_0$ = 10μM, pH_0 = 9.0, T = 25°C, F_{air} = 0.8 L min^{-1}.

Fig. 3: Effect of oxygen on PARA degradation. Condition: $[PARA]_0$ = 10μM, $[Co(II)]_0$ = 0.1 mM, $[Na_2SO_3]_0$ = 1.0 mM, pH_0 = 9.0, T = 25°C, F_{air} = 0.8 L min^{-1}.

Fig.4: Effect of radical scavenger of EtOH on PARA degradation.
Condition: $[PARA]_0$ = 10μM, $[Co(II)]_0$ = 0.1 mM, $[Na_2SO_3]_0$ = 1.0 mM, pH_0 = 9.0, T = 25°C, F_{air} = 0.8 L min^{-1}.

Fig. 5: Effect of heterogeneous catalyst CoO react with S(IV) to degrade PARA.
Condition: $[PARA]_0$ = 10μM, $[Na_2SO_3]_0$ = 1.0 mM, pH_0 = 9.0, T = 25°C, F_{air} = 0.8 L min^{-1}.

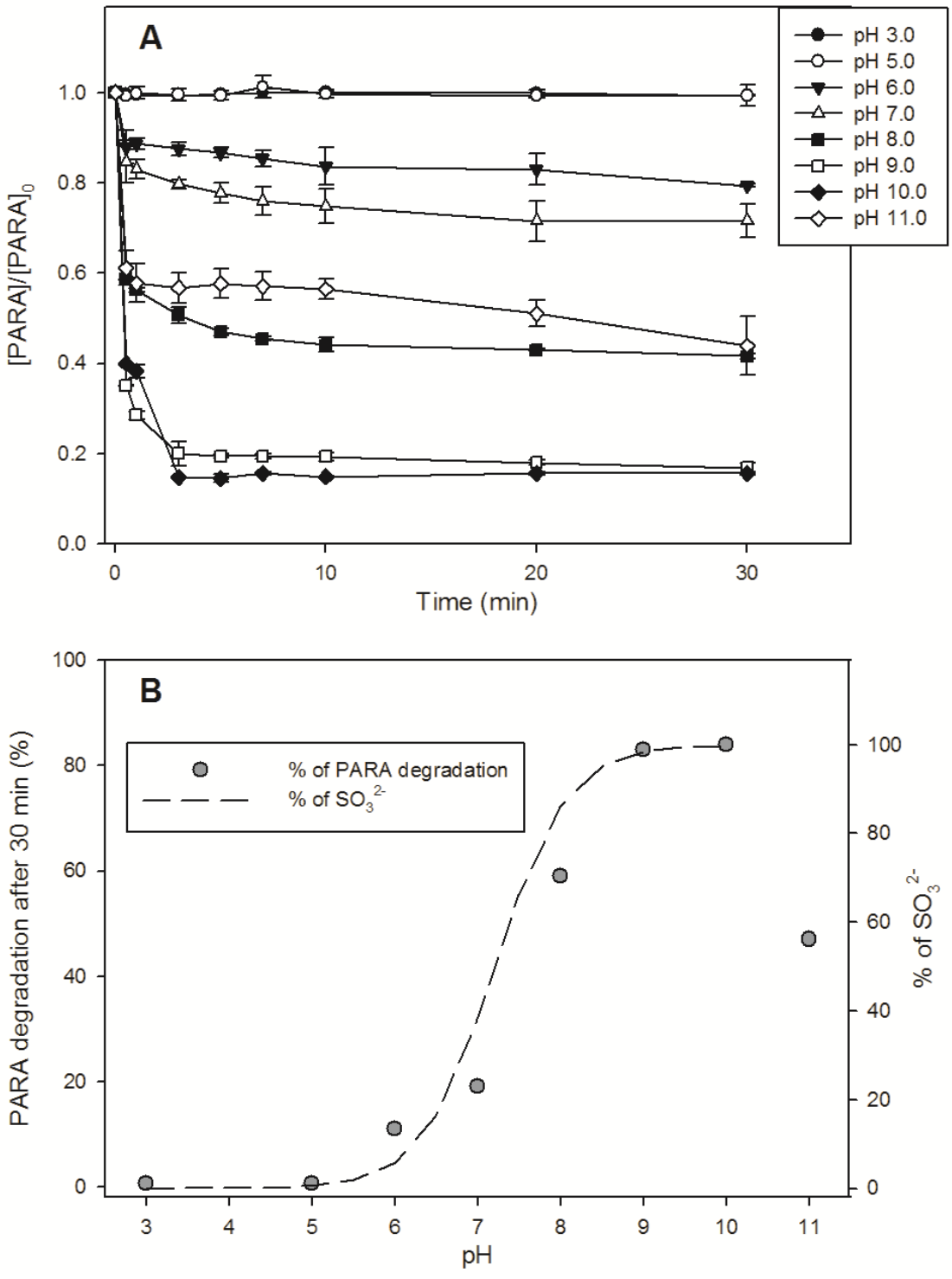
A
pH 3.0
pH 5.0
pH 6.0
pH 7.0
pH 8.0
pH 9.0
pH 10.0
pH 11.0
[PARA]/[PARA]0
Time (min)
B
% of PARA degradation
% of SO3 2-
PARA degradation after 30 min (%)
% of SO3 2-
pH

Fig. 1

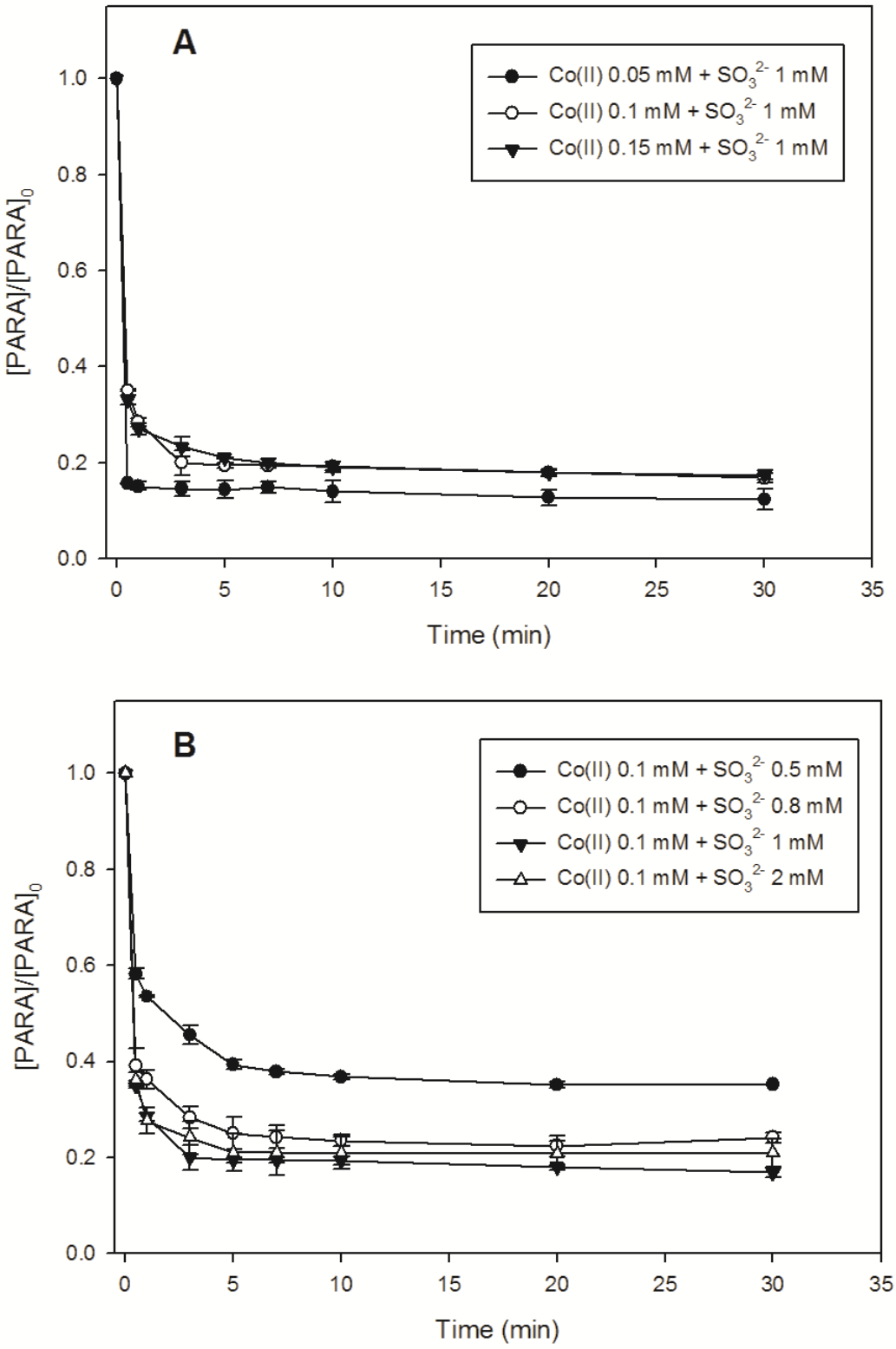
A
Co(II) 0.05 mM + SO_3^{2-} 1 mM
Co(II) 0.1 mM + SO_3^{2-} 1 mM
Co(II) 0.15 mM + SO_3^{2-} 1 mM
[PARA]/[PARA]$_0$
Time (min)
B
Co(II) 0.1 mM + SO_3^{2-} 0.5 mM
Co(II) 0.1 mM + SO_3^{2-} 0.8 mM
Co(II) 0.1 mM + SO_3^{2-} 1 mM
Co(II) 0.1 mM + SO_3^{2-} 2 mM
[PARA]/[PARA]$_0$
Time (min)

397

398 **Fig. 2**

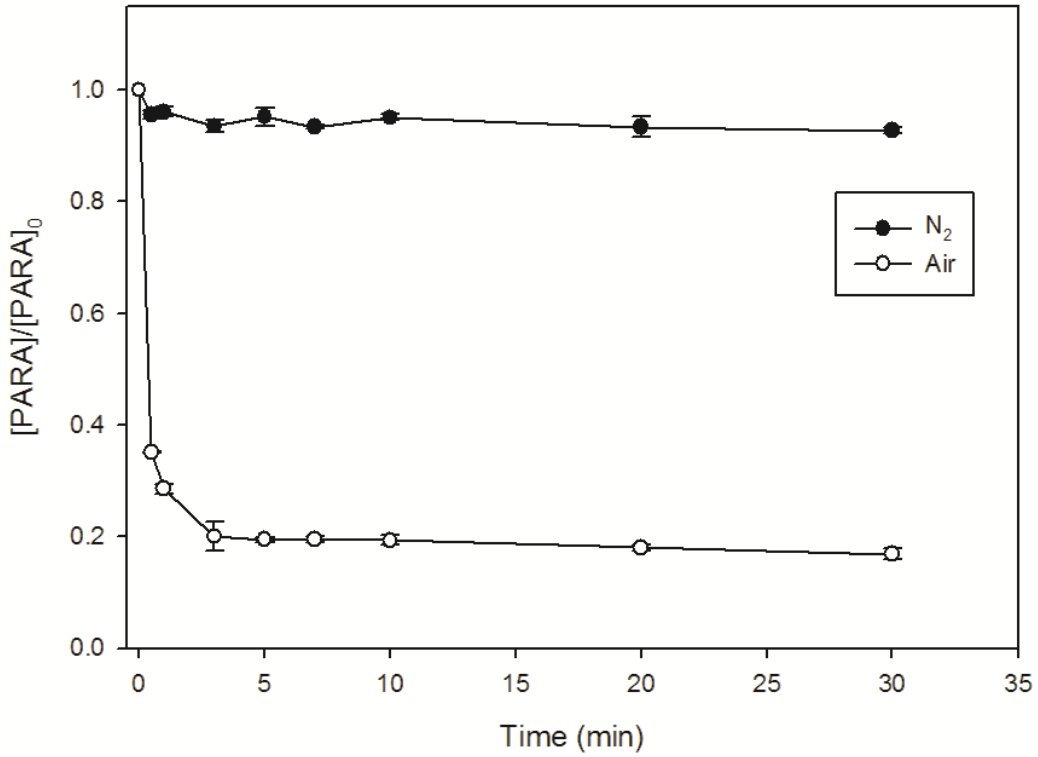

399

400 **Fig. 3.**

401

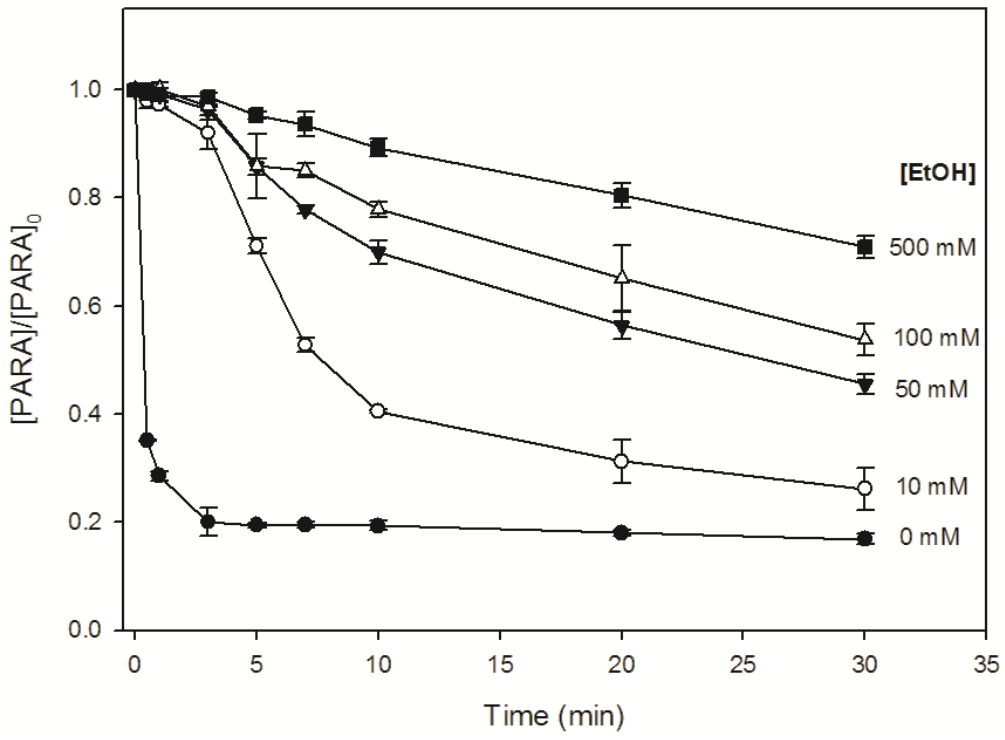

402

403 **Fig.4.**

404

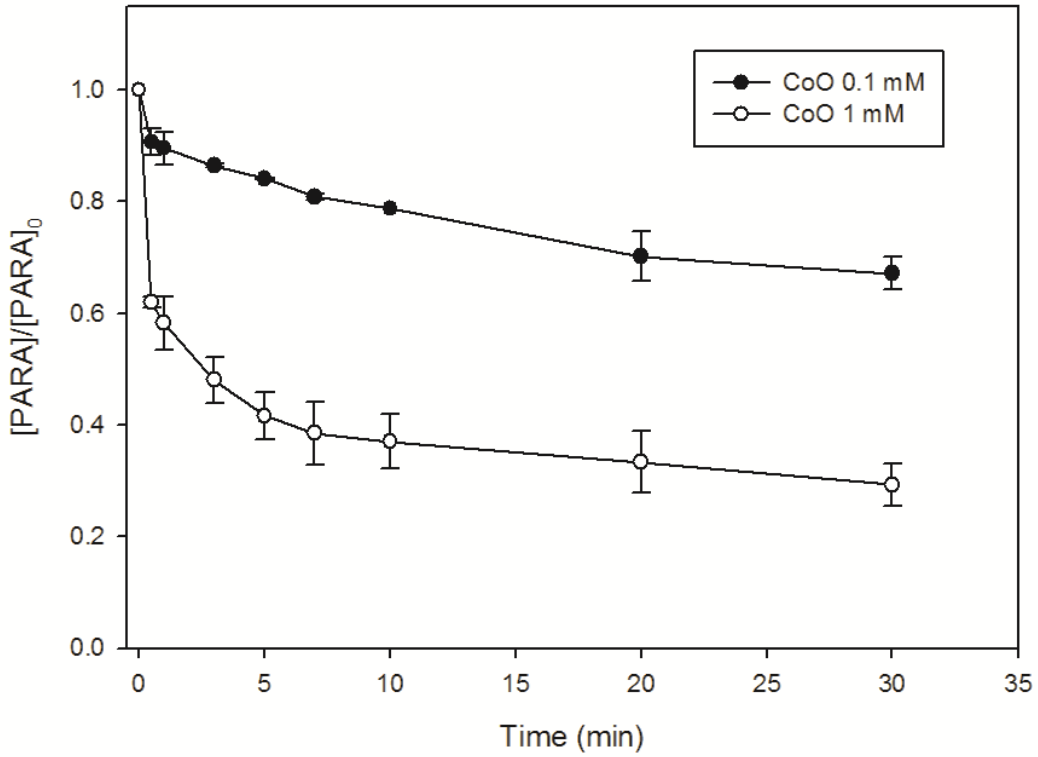

405

406 **Fig. 5**

407

408

Supplementary material

Rapid Oxidation of Organic Contaminants by Cobalt(II) Catalyzed Sulfite at Alkaline pH

Yanan Yuan[1,2], Dan Zhao[1], Jinjun Li[1], Feng Wu[1*], Marcello Brigante[2], Gilles Mailhot[2*]

[1] Department of Environmental Science, School of Resources and Environmental Science, Wuhan University, Wuhan, 430079, China.

[2] Université Clermont Auvergne, CNRS, SIGMA Clermont, Institut de Chimie de Clermont-Ferrand, F-63000 Clermont–Ferrand, France.

Corresponding Authors: Feng Wu (fengwu@whu.edu.cn) and Gilles Mailhot (gilles.mailhot@uca.fr)

Preliminary experiment using Co(II)-S(IV)

A typical degradation of Paracetamol by three different kinds of system (only Co(II), only sulfite(S(IV), Co(II)+S(IV)) is presented in Fig.S0. The result showed that when the experiment conducted in the presence of S(IV) without any catalyst, negligible change in paracetamol concentration was observed. A similar trend was also achieved in the experiment by only using Co(II) even after being centrifuged for 15 min at 9000 rpm. There was no precipitation occurred, which illustrated that there is no adsorption in this system and neither S(IV) nor Co(II) added to the reagent had an effect on Paracetamol. However, when both S(IV) and Co(II) were in solution, Paracetamol can be degraded to more than 80% in 10 min. These results suggest that Paracetamol degradation depends heavily on the reaction between S(IV) and Co(II), it proceeded only when S(IV) and Co(II) were present.

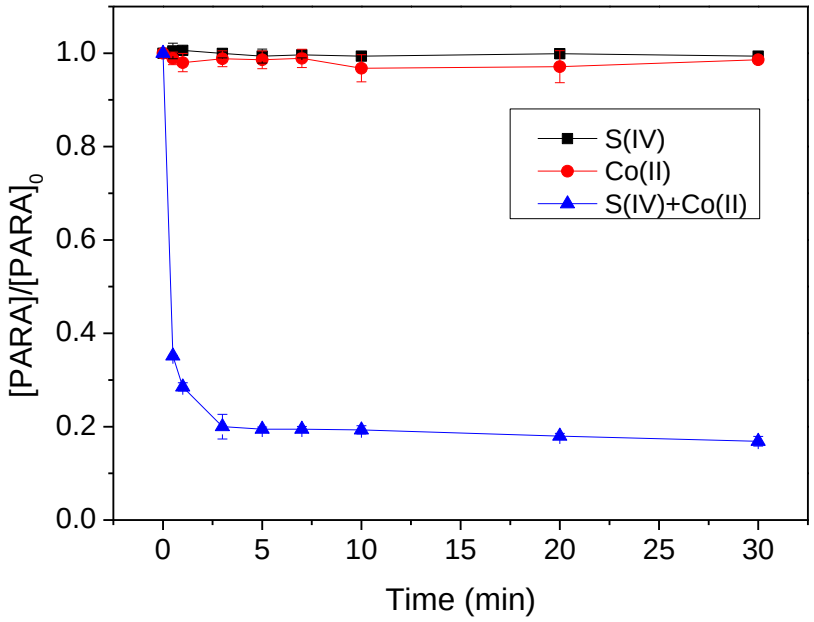

436

437 **Fig.S0** The effect of control experiments under various conditions on paracetamol
438 degradation. Condition: $[PARA]_0$ = 10μM, $[Co(II)]_0$ = 0.1 mM, $[Na_2SO_3]_0$ = 1.0
439 mM, pH_0 = 9.0, T =25°C, F_{air} = 0.8 L min^{-1}.

440

441

UV spectra of the reaction solution

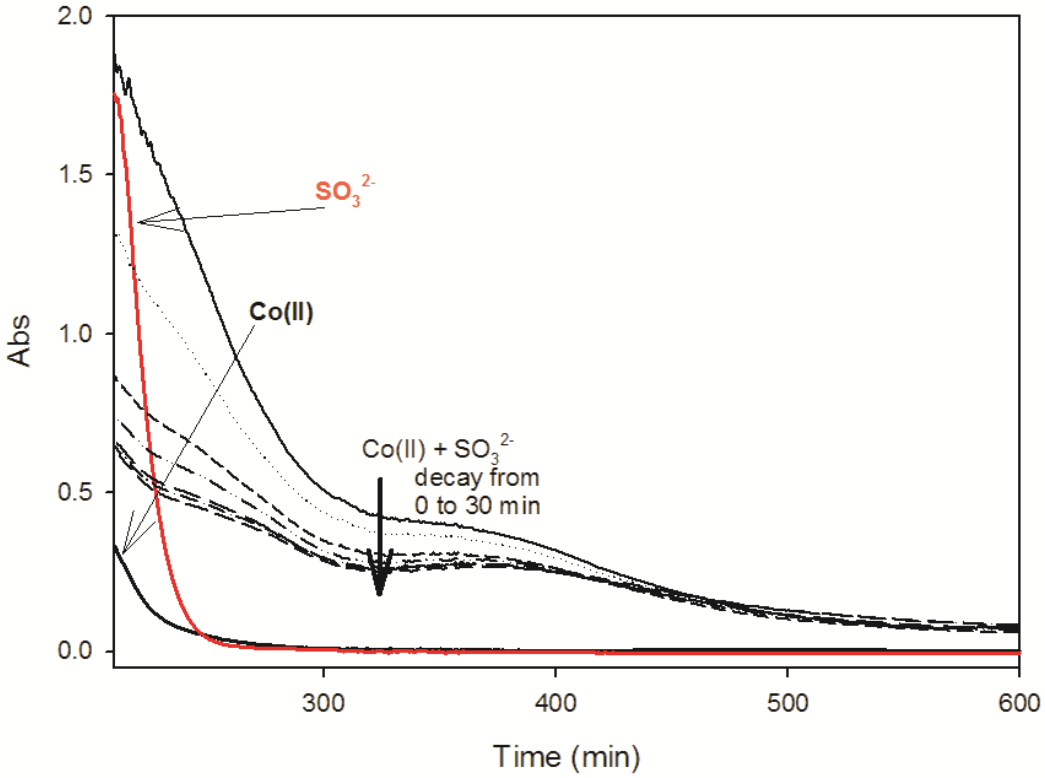

Fig. S1. UV–vis spectra of reaction solution at specific time intervals during the reaction. Conditions: $[Co(II)]_0$ = 0.1 mM, $[Na_2SO_3]_0$ = 1.0 mM, pH_0 = 9.0, T =25°C, F_{air} = 0.8 L min^{-1}.

Cobalt(II) quantification

The calibration of Cobalt(II) was measured by preparing a series of standard solutions, firstly , 5 mL cobalt(II) and 1 mL NH_4SCN(566g/L) was added to a 10 mL centrifuge tube and hand shaken for 1 min, then another 4 mL pure MIK was added to the mixture, and ultrasonic shaking for 1min and equilibrating until stratication occurred. Using the UV-Vis spectrophotometer for the absorbance at 620 nm for the upper layer complex which containing Cobalt(II). The calibration curve is presented in Fig. S2a.

The calibration equation is:

$$[Co^{2+}]\ (M) = (6.77\times10^{-4} \times Abs_{620\ nm}) - 7.02\times10^{-6}$$

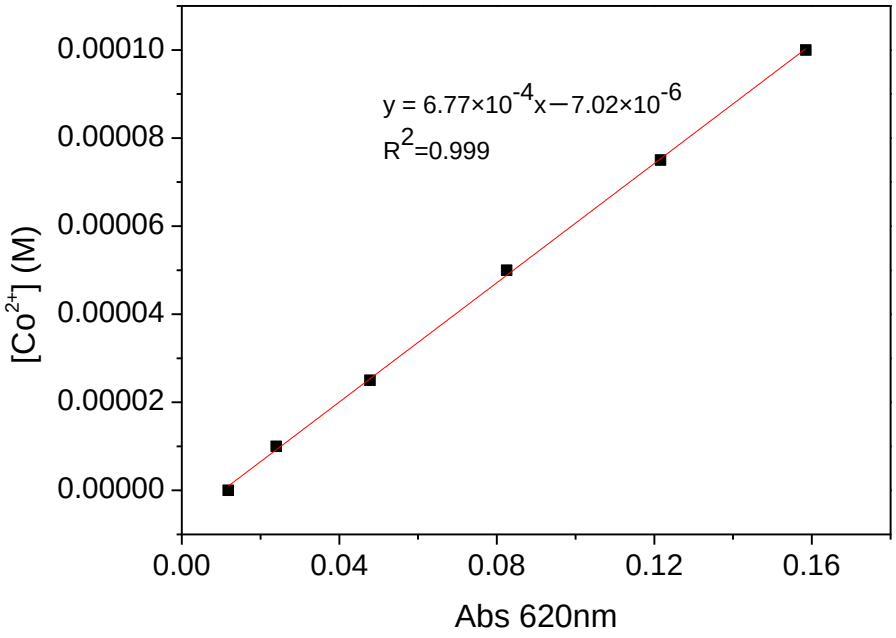

Fig.S2. Co(II) concentration vs Abs at 620 nm using described method

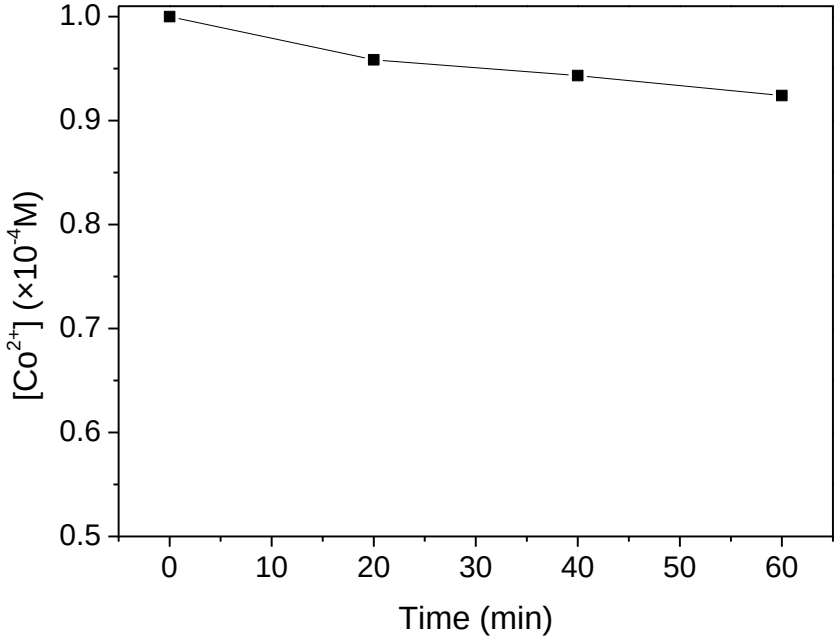

Fig. S3. Co(II) concentration during the reaction.

Condition: $[PARA]_0$ = 10μM, $[Co(II)]_0$ = 0.1 mM, $[Na_2SO_3]_0$ = 1.0 mM, pH_0 =

9.0, T =25°C, F_{air} = 0.8 L min^{-1}.

The determination of second order rate constants of sulfate radical and PARA

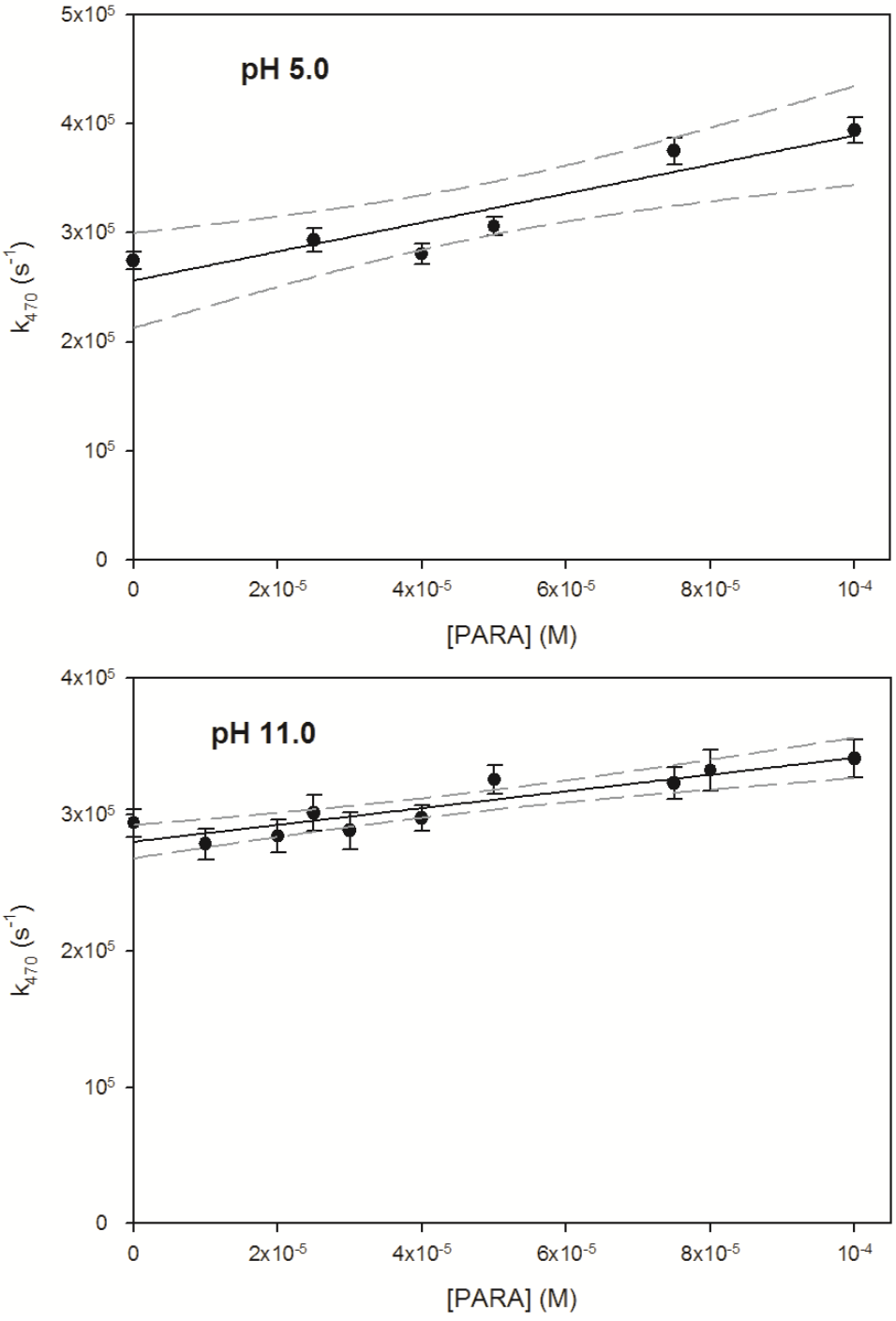

Fig. S4 : Pseudo-first order decay of sulfate radical monitored at 470 nm *vs* PARA concentration for molecular (pH 5.0) and deprotonated form (pH 11.0).solid line represents the linear fit of the experimental data and the dashed lines denote the 95% confidence interval of this fit.

The radical scavenger of TBA

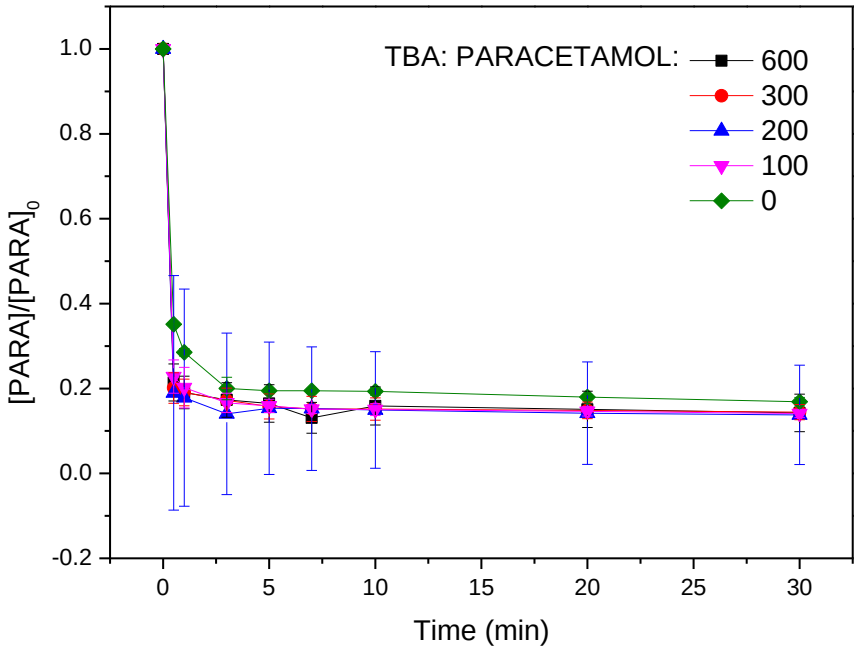

Fig. S5. Effect of TBA on paracetamol degradation.

Condition: $[PARA]_0$ = 10μM, $[Co(II)]_0$ = 0.1 mM, $[Na_2SO_3]_0$ = 1.0 mM, pH_0 = 9.0, T =25°C, F_{air} = 0.8 L min^{-1}.

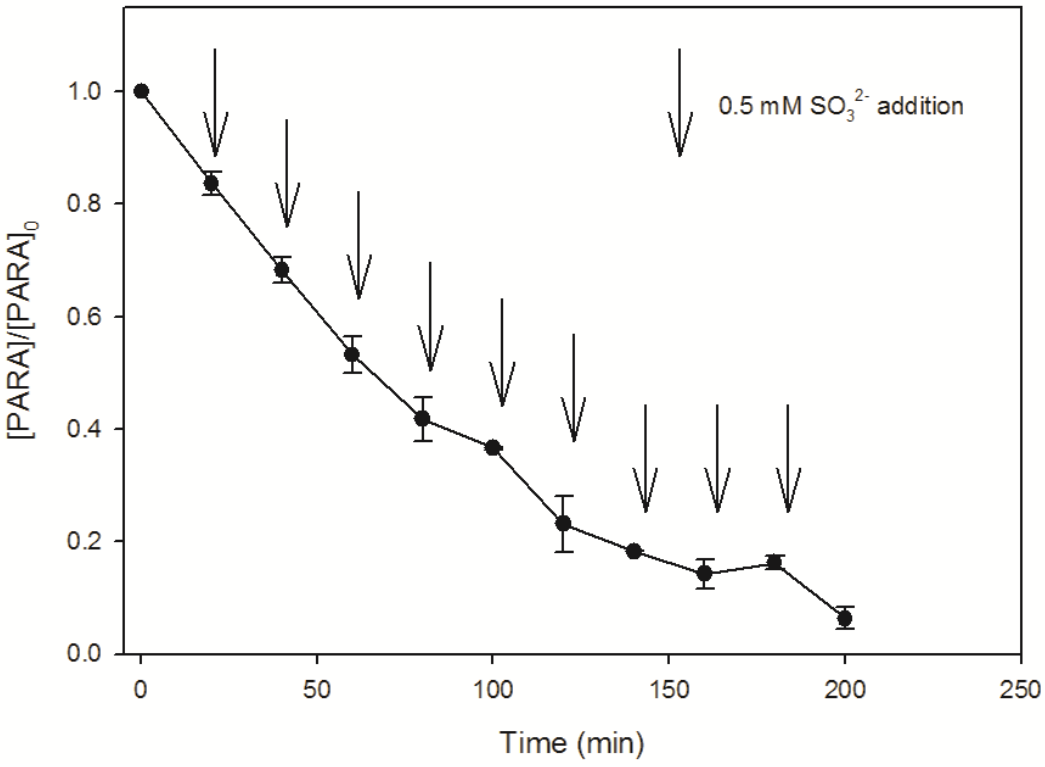

Fig. S6. Changes in paracetamol concentration over time in sequential experiments for the oxidation of paracetamol at high concentration. Initial conditions: $[PARA]_0$ = 500 μM, $[Co(II)]_0$ = 0.5 mM, $[Na_2SO_3]_0$ = 5.0 mM, pH_0 = 9.0, T =25°C, F_{air} = 0.8 L min^{-1}. Multiple additions of 0.5 mM S(IV) every 20 min.